On the fragmentation of benzene by multiphotoionization

Frank Rebentrost

Max-Planck-Institut für Quantenoptik, 8046 Garching bei München, West Germany

Avinoam Ben-Shaul

Department of Physical Chemistry, The Hebrew University, Jerusalem, Israel
(Received 4 September 1980; accepted 15 October 1980)

The MPI fragmentation of benzene is analyzed on the basis of experimental data and the dissociation dynamics of $C_6H_6^+$ at low excess energies. A multiple fragmentation mechanism with branchings is discussed in which vibrational energy is pumped into the $C_6H_6^+$ ground state by photon absorption and subsequent radiationless transitions. Calculations are performed for a statistical, products phase space model and show remarkably good agreement with the experimentally observed fragment patterns vs laser intensity. About 60 eV/molecule are required to make C^+ the most abundant ion, if all the energy were initially present in the $C_6H_6^+$. By RRKM estimates of the $C_6H_6^+$ decomposition rate it is concluded that such an assumption is not realistic and a model with multiple absorption and fragmentation steps applies.

I. INTRODUCTION

Extensive fragmentation following multiphotoionization (MPI) of polyatomic organic molecules has been observed recently.[1-8] The fragmentation patterns strongly depend on the laser intensity and can differ markedly from those obtained in photoionization (PI), photoelectron spectroscopy (PES), chemical activation (CA) by charge transfer, or electron impact (EI). In the case of benzene and other polyatomics the most striking feature is the occurrence of many small ions which indicates that much more energy is routed into the fragmentation than in the aforementioned methods. While in PI, CA, and EI the fragmentation essentially terminates at the C_4 and C_3 level, the C^+ ion becomes the most abundant fragment in MPI at laser intensities of the order of 100 MW/cm^2.

Here we discuss the possible mechanism for this new type of fragmentation on the basis of the presently available experimental information, thermochemical data, and a model calculation. Certainly, one would like to know whether the MPI fragmentation of benzene or other polyatomic molecules differs principally by its mechanism from the one applying, for example, to the CA or PI fragmentation. Experiments with time-delayed and multicolored pulses indicate that MPI fragmentation occurs in two steps: (1) ionization of benzene and (2) subsequent absorption of photons by the ions leading to their fragmentation. A point of particular interest is whether only the parent ion $C_6H_6^+$ absorbed all the laser radiation needed for fragmentation or, possibly, some of the intermediates absorb too. From the kinetic time scales for absorption, ionization, radiationless transitions, and fragmentation characterizing present MPI experiments, we reach the conclusion that the latter mechanism applies. We also make an attempt to identify the absorbing ions. In a more quantitative fashion, a statistical model is used for predicting the mass and energy distributions of the species generated along a fragmentation tree originating with a highly excited parent ion. The calculation also strongly supports a mechanism involving secondary absorption and is capable of accounting for the unlikeliness of certain ions like CH^+ which are not seen in MPI experiments. We also obtain a surprisingly good quantitative agreement with the observed mass patterns and in particular their dependence on laser intensity. It turns out that most of our results remain at least qualitatively valid when accounting for absorption by any secondary ions.

II. FRAGMENTATION OF BENZENE BY NON-MPI METHODS

The fragmentation of benzene ions has received much interest in the past. It is now well established that the primary fragmentation paths with threshold energies E^0 around 4 eV are

$$C_6H_6^+ \rightarrow C_6H_5^+ + H\,, \quad E^0 \cong 3.6\ \text{eV}\,, \tag{1.1}$$

$$\rightarrow C_6H_4^+ + H_2\,, \quad E^0 \cong 4\text{–}5\ \text{eV}\,, \tag{1.2}$$

$$\rightarrow C_4H_4^+ + C_2H_2\,, \quad E^0 \cong 4.2\ \text{eV}\,, \tag{1.3}$$

$$\rightarrow C_3H_3^+ + C_3H_3\,, \quad E^0 \cong 4.4\ \text{eV}\,. \tag{1.4}$$

Earlier investigations by Andlauer and Ottinger,[9] Eland and Schulte,[10] and others seemed to favor an explanation by which hydrogen abstraction and C–C bond breaking form noncompeting channels in the sense of the RRKM or QET theories. This could have been the result of two noncommuting electronic states of the benzene ion (e.g., the $X\,^2E_{1g}$ and $^2A_{2u}$ states). More recently, new experimental data obtained by the photoion–photoelectron coincidence (PIPECO) technique as well as their successful interpretation by a RRKM model led Baer and coworkers[11] to the conclusion that all these fragmentations may in fact start from the electronic ground state of $C_6H_6^+$. This is also in agreement with the rare observation of fluorescing polyatomic ions due to rapid radiationless transitions taking place at rates of the order of 10^{12} sec^{-1} in the case of benzene ions.[12]

Breakdown graphs of benzene ions[13] obtained by charge exchange with ions of varying recombination energies cover the range of internal excitation energies up to about 15 eV (Fig. 1). Here secondary fragmentations play an increasing role and in addition lead to the ions $C_4H_3^+$, $C_4H_2^+$, C_4H^+ and $C_3H_2^+$, C_3H^+ from $C_4H_4^+$ and $C_3H_3^+$,

 0021-9606/81/063255-10$01.00

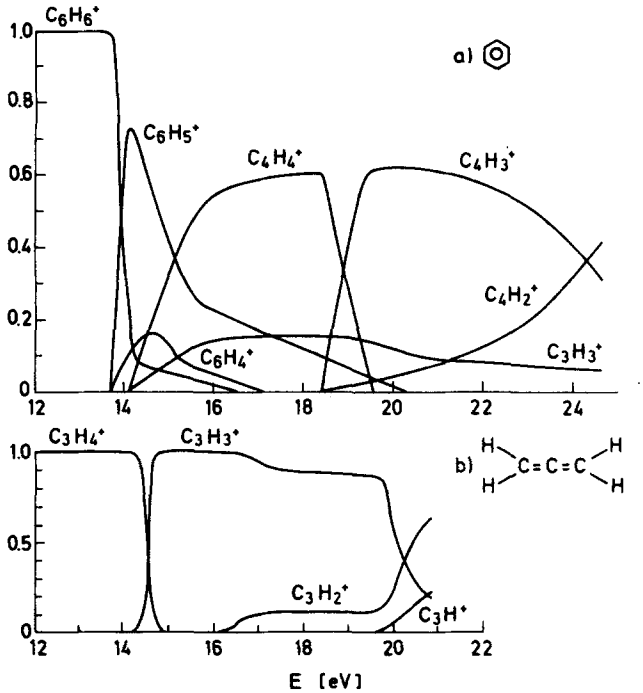

FIG. 1. (a) Breakdown diagrams of benzene by charge change[13] and (b) allene by photoionization.[15] In (b) the energy axis is shifted to make the appearance potential of $C_3H_3^+$ equal in cases (a) and (b).

respectively. A general observation is that H_2 eliminations of $C_6H_6^+$, $C_4H_4^+$, and $C_3H_3^+$ seem to occur with rather low rates when compared with abstractions of a single H atom, even though their thresholds are usually about the same. This may be due to the rigid and therefore statistically unfavorable four-center transition complex required for H_2 eliminations. There is also some indication of further C–C bond breaking leading to the ions $C_2H_3^+$ and $C_2H_2^+$ by reactions like $C_6H_6^+ - C_4H_4^+ - C_2H_2^+$ with the elimination of two acetylene molecules.

Extrapolation of this picture to somewhat higher excitation energies is possible by using information contained in the breakdown graphs of smaller hydrocarbon compounds, e.g., vinylacetylene $HC{\equiv}C{-}CH{=}CH_2$, diacetylene $HC{\equiv}C{-}C{\equiv}CH$, cyclopropene (Ref. 14) C_3H_4, allene (Ref. 15) $CH_2{=}C{=}CH_2$ [Fig. 1(b)], propyne (Ref. 16) $HC{\equiv}C{-}CH_3$, or acetylene (Refs. 17 and 18) $HC{\equiv}CH$. Experience with organic ions has shown that quite often rapid hydrogen scramblings and isomerizations occur prior to unimolecular decay. In the case of isomers like allene, propyne, and cyclopropene this explains the almost identical behavior with respect to fragmentation though some specific behavior remains.[19] In the case of $C_2H_2^+$ one observes H abstraction and H_2 elimination but also C–C bond breaking. Of interest is the fact that the CH^+ channel is preferred to the formation of C^+, just the opposite being the case in the MPI fragmentation of benzene. Most likely, the electronically excited acetylene ions produced by charge transfer cannot relax rapidly enough to the electronic ground state and the fragmentation to CH^+ is a property of an excited state.[20] This may be rationalized by the large excitation gap (5 eV), the small size, and the rigidity of the molecular ion.

Similar evidence is obtained from the fragment distributions in EI mass spectrometry.[21–23] Here the observed mass distributions also reflect the rather broad range of energies in the parent ions obtained by collisions with energy-rich electrons (~ 70 eV).

III. CHARACTERISTICS OF MULTIPHOTOIONIZATION

Table I summarizes operating conditions under which MPI and fragmentation of benzene have been demonstrated by various research groups. In the work with UV excimer lasers by Reilly and Kompa[2] the ionization limit is reached by the absorption of only two photons through the intermediate $^1B_{2u}$ and $^1B_{1u}$ states. Due to the high powers, the total ion yield saturates because of depletion in the benzene ground state. With visible dye lasers of similar intensity, the total ion yield varies roughly with I^2, due to a rate determining two photon excitation of a *"gerade"* vibronic state of benzene. As shown by Boesl *et al.*[6] with a second time-delayed laser pulse, the excess energy required for fragmentation is obtained by absorption starting from the benzene ion. The important consequence is therefore that ionization and fragmentation are in effect decoupled and the detailed mechanism of ionization is rather immaterial for an understanding of the fragmentation itself. Thus, while in MPI the function of the laser is twofold in providing energy for ionization and subsequent fragmentation, it should be possible and challenging to investigate the laser fragmentation of benzene ions independent of the ionization step. The assumption that the fragmentations result from pumping the ions shall also be accepted here. It would contradict interpretations in which the fragmentations occur via a tree of autoionizing states of the neutral,[4,7] i.e., the laser pumps a manifold of states in benzene rather than in the ion.

TABLE I. Typical experimental conditions used in MPI laser fragmentation of benzene.

Authors	Laser	FWHM (nsec)	E_{phot} (eV)	Intensity (MW/cm^2)	Fluence (J/cm^2)	Remarks
Reilly and Kompa[2]	KrF	20	5.0	$\lesssim 300$	$\lesssim 6$	Ion yield saturates
	ArF	12	6.4	$\lesssim 160$	$\lesssim 2$	
Zandee and Bernstein[4]	Dye	5–6	3.1–3.3	$\lesssim 1000$	$\lesssim 6$	Ion yield $\propto I^2$
Boesl *et al.*[6]	Dye	8	>2.4	$\lesssim 400$	$\lesssim 3$	
	Second harmonic		5.0	~3		Only $C_6H_6^+$, no fragments

TABLE II. Heats of formation[24,25] ΔH^f of relevant ions and neutrals.

Ion	ΔH^f (kcal/mole)[a]	A. P. (eV)[b]
$C_6H_6^+$	233.1(19.8)	9.25
$C_6H_5^+$	268. (79.)	13.0
$C_6H_4^+$	352. (164.)	14.4
$C_6H_3^+$	455.	21.1
$C_5H_6^+$	229.	16.5
$C_5H_5^+$	260.	16.6
$C_5H_3^+$	368.	16.6
C_5^+	535.	21.6
$C_4H_6^+$	235. (26.33)	18.0
$C_4H_5^+$	240.	14.5
$C_4H_4^+$	278. (72.8)	13.6
$C_4H_3^+$	307.	15.3
$C_4H_2^+$	347.6(113.)	14.8
C_4H^+	386.	15.0
C_4^+	526.5(243.2)	21.1
$C_3H_6^+$	229. (4.88)	17.6
$C_3H_5^+$	226. (40.6)	19.7
$C_3H_4^+$	269. (44.32)	19.3
$C_3H_3^+$	229. (80.35)	13.7
$C_3H_2^+$	357.	16.6
C_3H^+	381.	17.4
C_3^+	480. (196.)	20.2
$C_2H_6^+$	249. (−20.24)	20.5
$C_2H_5^+$	219. (25.7)	21.4
$C_2H_4^+$	257. (12.49)	15.2
$C_2H_3^+$	269. (65.)	18.0
$C_2H_2^+$	257. (54.34)	16.1
C_2H^+	399. (114.)	21.6
C_2^+	476. (199.)	20.9
CH_4^+	275. (−17.88)	21.9
CH_3^+	262. (33.2)	21.6
CH_2^+	334. (93.7)	22.1
CH^+	387. (142.4)	21.8
C^+	429.6(171.29)	21.9
H_2^+	355.7(0.)	21.7
H^+	366. (52.10)	18.5

[a] ΔH^f for neutrals in parentheses.

[b] Minimal appearance potentials (A. P.) are calculated for the general fragmentation tree constructed from all possible branchings $C_mH_n^+ \rightarrow C_kH_l^+ + C_\xi H_\gamma$ when ΔH^f values were available.

The breakdown graphs discussed in Sec. II give evidence that the primary fragments $C_4H_4^+$ and $C_3H_3^+$ undergo consecutive loss of H or H_2. To explain the ample occurrence of C_2 fragments and of C^+ in MPI, one can investigate the possible fragmentation paths on the basis of thermochemical data. With the heats of formation for the relevant ions and neutrals, theoretical appearance potentials for the ions may be calculated for any chosen fragmentation path. This was done by considering first the most general fragmentation tree starting with $C_6H_6^+$ that can be constructed from the thermochemical data of Table II. It consists of approximately 10^5 different paths terminating with either C^+ or H^+. For each ion one obtains a minimum appearance potential, as displayed in Table II. Clearly, the rather similar appearance potentials for H^+, C^+, and CH^+ (all around 20 eV, corresponding to 11 eV excess energy of $C_6H_6^+$) do not account for the prominent C^+ formation and the absence of ions like H^+, H_2^+, CH^+, and others in MPI. As will be shown in Sec. V, these facts follow very naturally from a statistical model.

Several time scales will affect the fate of the primary ions. Among them, most important are the ones due to absorption of photons by $C_6H_6^+$ and its overall decomposition rate $k_d(E)$. With the upper limits of the intensities given in Table I, one expects for instance in the case of the KrF laser the photon absorption rates to be in the range $(4\times10^8)-(4\times10^{10})$ sec^{-1} when the absorption cross section of $C_6H_6^+$ is assumed to be in the range 0.01–1 Å^2. In agreement with the findings of Boesl *et al.*[6] the direct ionization (10^{-14}–10^{-15} sec) and typical autoionizations (10^{-12}–10^{-13} sec) occur much more rapidly.

By the fact that the radiationless transition rate is of the order of 10^{12} sec^{-1}, all energy pumped into an electronically excited state immediately appears as nuclear excitation of the ground state. Such a high internal conversion rate would also explain why no doubly charged ions have been seen in MPI.

For an estimate of the time scale of the primary fragmentation steps we have calculated the decomposition rate of $C_6H_6^+$ into the $C_6H_5^+$, $C_4H_4^+$, and $C_3H_3^+$ channels by extending a calculation by Baer *et al.*[11] to larger excess energies (Fig. 2). Of particular interest is the excitation energy at which the decomposition and the absorption rates of $C_6H_6^+$ become equal. This energy is approximately 8–10 eV and corresponds to 50% probability $[=k_{abs}/(k_{abs}+k_d)]$ for absorption of another photon. In the case of a KrF laser the benzene ion will therefore obtain an excess energy of 10–15 eV by absorption of 2–3 photons. With respect to the minimal appearance potentials of Table II, this is not far from the minimum energy required to form all observed fragment ions. On the other hand, certainly a higher excess energy is needed to drive efficiently those paths that ultimately lead to C^+ because of considerable energy lost as internal energy of the neutrals and as kinetic shifts. The important conclusion from our rate calculation is then that at least some of the fragments must also absorb radiation. This supports a *multiple absorption/fragmentation* mechanism (MAF) as suggested in the work by Reilly and Kompa[2] for different reasons. Such a mechanism can be contrasted with an *absorption/multiple fragmentation* (AMF) mechanism, where it is assumed that only the parent ion absorbs energy from the radiation field. Both the AMF and MAF models can be put on a statistical basis to be discussed for the AMF case in Sec. IV.

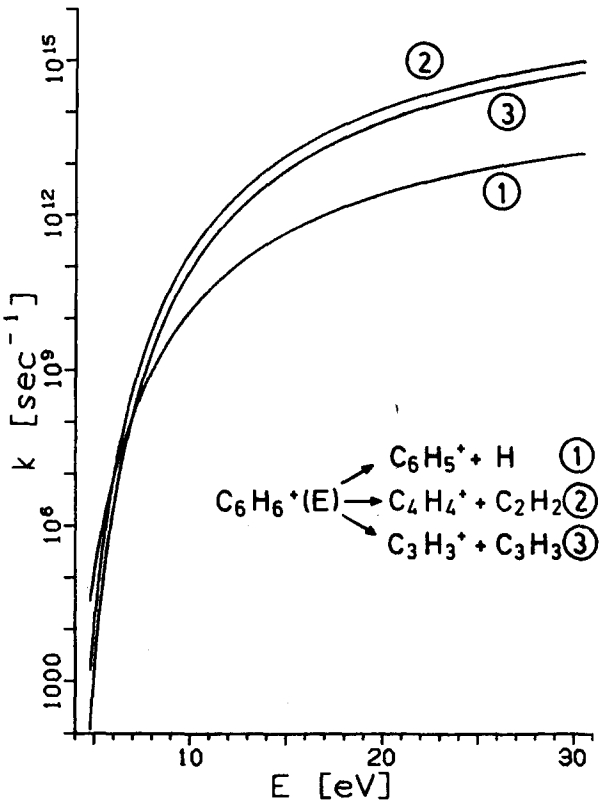

FIG. 2. RRKM rates for the fragmentation of $C_6H_6^+(E)$ to $C_6H_5^+$, $C_4H_4^+$, and $C_3H_3^+$ as functions of excess energy E.

At present it is not known to what extent the fragments formed under MPI conditions continue to absorb photons. Unfortunately, there is too little spectroscopic data on the ions available to discuss this question in a quantitative manner. Some crude information on the location of the electronic terms may be obtained by semiempirical methods (Hückel, PPP, CNDO-S). In general, ionic spectra may differ considerably from the corresponding neutral ones because of the possibility of unfilled bonding orbitals leading to additional bands in the visible region.[26] Already by the Hückel orbital energies of benzene one understands the occurrence of a low-lying $X\,^2E_{1g} \rightarrow {}^2A_{2u}$ transition of $\pi-\pi$ character in the benzene ion ($a_{2u}^2 e_{1g}^3 \rightarrow a_{2u} e_{1g}^4$; $\Delta\epsilon = -\beta$) in addition to $\pi-\pi^*$ transitions ($a_{2u}^2 e_{1g}^3 \rightarrow a_{2u}^2 e_{1g}^2 e_{2u}$; $\Delta\epsilon = -2\beta$) in the UV region. Similar behavior is expected for $C_6H_5^+$ and $C_6H_4^+$. Also, linear $C_6H_6^+$ structures, e.g., $CH_3-C\equiv C-C\equiv C-CH_3^+$, are known to have absorption bands in the visible region.[27]

For the methylen cyclopropene structure of $C_4H_4^+$ the $\pi-\pi$ transition $[b_1(1)^2 b_2(2) \rightarrow b_2(1) b_2(2)^2$; $\Delta\epsilon = -1.86\beta]$ is at even larger energy than the lowest $\pi-\pi^*$ transition $[b_2(1)^2 b_2(2) \rightarrow b_2(1)^2 a_2$; $\Delta\epsilon = -1.31\beta]$. For the less likely cyclobutadiene structure of $C_4H_4^+$ the Hückel calculation predicts $\pi-\pi$ and $\pi-\pi^*$ transitions with $\Delta\epsilon = -2\beta$, i.e., in the UV. The cyclopropenyl cation $C_3H_3^+$ has the aromatic ground state configuration $a_2''^2$ and the $\pi-\pi^*$ promotion requires a $\Delta\epsilon$ of -3β. On the other hand, for one of the smaller fragments, namely, the linear diacetylene cation $C_4H_2^+[\Delta\epsilon(^2\Pi_u - {}^2\Pi_g) = 2.43$ eV], a low-lying transition is known.[27] Very likely the same is true for other structures of the type C=C–C≡C and C≡C–C≡C, making the C_4 fragments possible candidates for single-photon absorption in the visible range. Absorption of visible light by C_3 and smaller fragments would necessarily be a two-photon process, if it is essential for MPI at all.

A possible consequence of an MAF mechanism could be specificity of the fragmentation with respect to the laser wavelength. In the rather wide range 1930 to 5400 Å this does not seem to be the case, since the observed fragmentation patterns are all qualitatively alike. On the other hand, it is also not likely that all fragmenting intermediates are formed during the laser pulse. If for instance this were the case for $C_2H_2^+$, one expects the formation of CH^+. Certainly, the photons of the KrF and ArF lasers could excite $C_2H_2^+$ while this is not the case for the visible lasers employed. Since, independent of the laser frequency, CH^+ was not observed, the conclusion would be that $C_2H_2^+$ is formed with delay times larger than 20 nsec.

IV. STATISTICAL MODEL FOR MULTISTEP FRAGMENTATION

Let $P_{ij}(E_i, E_j)dE_j$ denote the probability that an ion I_i^+ with internal energy E_i will fragment into a smaller ion I_j^+ with internal energy in the range $E_j, E_j + dE_j$ and into a complementary neutral N_{ij}. Clearly, $P_{ij}(E_i, E_j)$ vanishes for $E_i < E_{ij}^0$ and $E_j > E_i - E_{ij}^0$, where E_{ij}^0 is the energetic barrier of the process $I_i^+ \rightarrow I_j^+ + N_{ij}$. The energy balance

$$E_i = E_{ij}^0 + E_j + E_{ij} + \epsilon_t \tag{4.1}$$

then also contains contributions E_{ij} from the internal energy of the neutral and the relative translational energy ϵ_t of the products. In the following we shall not be interested in the partitioning of the residual energy $\overline{E_{ij}} = E_{ij} + \epsilon_t = E_i - E_{ij}^0 - E_j$ since it does not affect the further fragmentation of the ion I_j^+. Using $k_{ij}(E_i, E_j)$ for the rate of producing ion I_j^+ with internal energy E_j from the parent ion I_i^+ with energy E_i, we have

$$P_{ij}(E_i, E_j) = k_{ij}(E_i, E_j)/k_i(E_i)\ , \tag{4.2}$$

where

$$k_i(E_i) = \sum_j \int_0^{E_i - E_{ij}^0} dE_j\, k_{ij}(E_i, E_j) = \sum_j k_{ij}(E_i)\ . \tag{4.3}$$

Here $k_{ij}(E_i)$ is the total (E_j-integrated) rate constant into channel j and $k_i(E_i)$ is the total fragmentation rate of ion I_i^+.

Equation (4.2) can also be rewritten as

$$P_{ij}(E_i, E_j) = F_{ij}(E_i) f_{ij}(E_i, E_j)\ , \tag{4.4}$$

where

$$F_{ij}(E_i) = k_{ij}(E_i)/k_i(E_i) \tag{4.5}$$

is the branching fraction of channel $i \rightarrow j$ and

$$f_{ij}(E_i, E_j) = k_{ij}(E_i, E_j)/k_{ij}(E_i) \tag{4.6}$$

is the internal energy distribution of the daughter ion I_j^+ following its formation from the parent ion $I_i^+(E_i)$. The normalization relations are

$$\sum_i \int_0^\infty dE_j\, P_{ij}(E_i, E_j) = \sum_j F_{ij}(E_i) = 1 \ , \tag{4.7}$$

$$\int_0^\infty dE_j f_{ij}(E_i, E_j) = 1 \ . \tag{4.8}$$

As described in the previous section, there are many fragmentation paths leading from the parent $C_6H_6^+$ ion to the smallest observed fragment C^+. Depending on the initial and intermediate energies, a particular fragmentation sequence may either continue or terminate at the level of any molecular ion. On a particular path γ, i.e., $I_1^+(E_1) \to I_2^+(E_2) \to \cdots \to I_2^+(E_i) \to I_j^+(E_j) \to I_k^+(E_k) \to \cdots$, with specified energies, the fragmentation cannot go beyond ion I_j^+ if the initial energy was such that

$$E_{12}^0 + \cdots + E_{ij}^0 < E_1 < E_{12}^0 + \cdots + E_{ij}^0 + E_{jk}^0 \ .$$

Taking $P_1(E_1)$ as the energy distribution of the parent ion I_1^+, the probability for obtaining I_j^+ on path γ is

$$p_j^\gamma = \int_0^\infty dE_1 P_1(E_1) \times \int_0^\infty dE_2 P_{12}(E_1, E_2) \cdots \int_0^\infty dE_i \int_0^{E_j^0} dE_j P_{ij}(E_i, E_j) \tag{4.9}$$

where E_j^0 refers to the minimal threshold for any further fragmentation of I_j^+. All upper integration limits apart from the last one in Eq. (4.9) can be extended to infinity since the P_{ij} will vanish if the energy balance cannot be satisfied. By summing over all paths involving j, we obtain the total probability for forming I_j^+ as

$$p_j = \sum_\gamma p_j^\gamma \ . \tag{4.10}$$

A convenient evaluation of the multiple integrations occurring in Eq. (4.9) can be done by exploiting the Markovian structure of the multistep fragmentation process. With the energy distribution $P_j(E_j)$ prior to fragmentation defined for all ions as

$$P_j(E_j) = \sum_\gamma \int_0^\infty dE_1 P_2(E_1) \times \int_0^\infty dE_2 P_{12}(E_1, E_2) \cdots \int_0^\infty dE_i P_{ij}(E_i, E_j) = \sum_{i' \to j} \int_0^\infty dE_{i'} P_{i'}(E_{i'}) P_{i'j}(E_{i'}, E_j) \ , \quad \int_0^\infty dE_j P_j(E_j) \le 1 \ , \tag{4.11}$$

one sees from the last line that the summation extends now only over those ions i' that lead to j in a single step. Since necessarily i' is a larger ion than its fragment j, all P_j can be calculated by single integrations starting with the parent ion I_1^+ and descending with respect to molecular size (or weight). The final p_j then are obtained as

$$p_j = \int_0^{E_j^0} dE_j P_j(E_j) \ . \tag{4.12}$$

As seen from Eqs. (4.9) and (4.12), any ion with sufficient energy to overcome a consecutive barrier is assumed to actually fragment. In practice, an upper limit for the lifetime of a fragmenting ion is of the order of 10^{-6} sec in conventional mass-spectrometric detection.[28]

The common approach for estimating $P_{ij}(E_i, E_j)$ in the theory of mass spectra[28-30] involves two stages: (1) The rate constants $k_{ij}(E_i)$ and hence by Eq. (4.5) the branching fractions $F_{ij}(E_i)$ are calculated according to RRKM theory; (2) the products energy distributions $f_{ij}(E_i, E_j)$ are determined by assuming that the available energy is distributed "microcanonically" (or in classical terms "equipartitioned") among the various degrees of freedom of the daughter ion and the complementary neutral. This form of energy partitioning is also known as the "prior" distribution[31] in the information theoretic approach to molecular dynamics. It is essentially also the products energy distribution predicted by the unimolecular variant[32] of phase space theory.[33,34] For unimolecular reactions the phase space theory may be regarded as a limiting case of RRKM theory assuming that the transition states are so loose that they become practically identical to the products.[35] Most ionic fragmentation reactions are believed to proceed via such loose transition complexes.[28] Hence, apart from minor differences the branching fractions $F_{ij}(E_i) \propto k_{ij}(E_i)$ calculated by RRKM, phase space, or the prior models are essentially all the same; in all cases the probability of each product channel j is proportional to its microcanonical weight (phase space volume). Thus, in the following and instead of combining two models, one for $F_{ij}(E_i)$ and the other for $f_{ij}(E_i, E_j)$, we shall adopt the microcanonical prior model for both.

In fact, the assumption of a microcanonical products distribution can be directly applied to $P_{ij}(E_i, E_j)$. This assumption implies

$$P_{ij}(E_i, E_j) = \alpha_{ij} \rho_j(E_j) \overline{\rho_{ij}}(E_i - E_{ij}^0 - E_j)/\Omega_i(E_i) \ , \tag{4.13}$$

with

$$\Omega_i(E_i) = \sum_j \alpha_{ij} \int dE_j\, \rho_j(E_j) \overline{\rho_{ij}}(E_i - E_{ij}^0 - E_j) = \sum_j \Omega_{ij} \ . \tag{4.14}$$

In these equations α_{ij} is the reaction path degeneracy, $\rho_j(E)$ the density of internal (vibrotational) states of $I^+(E)$, and $\overline{\rho_{ij}}(E)$ is the joint density of states for the internal degrees of freedom for the complementary neutral N_{ij} and the relative translational motion of the $I_j^+(E_j) + N_{ij}$ pair. As usual, $\overline{\rho_{ij}}$ is obtained as a convolution

$$\overline{\rho_{ij}}(E) = \int_0^E d\epsilon_t\, \rho_t(\epsilon_t) \rho_{ij}(E - \epsilon_t) \ , \tag{4.15}$$

where $\rho_t(\epsilon_t) = C_t \mu^{3/2} \epsilon_t^{1/2}$ is the translational density of states (μ is the reduced mass and C_t a constant) and ρ_{ij} is the density of internal states of the neutral. Note that the summation in Eq. (4.14) is extended over all product channels. The quantities of interest are therefore

$$F_{ij}(E_i) = \Omega_{ij}(E_i)/\Omega_i(E_i) \ , \tag{4.16}$$

$$f_{ij}(E_i, E_j) = \alpha_{ij} \rho_j(E_j) \overline{\rho_{ij}}(E_i - E_{ij}^0 - E_j)/\Omega_{ij}(E_i) \ .$$

Assuming that all products degrees of freedom share the energy available for distribution, harmonic vibrations, and classical rotations and translations, ρ_j and $\overline{\rho_{ij}}$ are approximated by

$$\rho_j(E) = g_j Q_j \frac{(E + a_j E_{0j})^{s_j + r_j/2 - 1}}{\Gamma(s_j + \frac{1}{2} r_j) \prod_{\alpha=1}^{s_j} h\nu_{\alpha j}}, \tag{4.17}$$

$$\overline{\rho_{ij}}(E) = C_i \bar{g}_j \bar{Q}_j \frac{(E + \bar{a}_j \bar{E}_{0j})^{\bar{s}_j + \bar{r}_j/2 + 1/2}}{\Gamma(\bar{s}_j + \frac{1}{2}\bar{r}_j + \frac{3}{2}) \prod^{\bar{s}_j} h\bar{\nu}_{\alpha j}}. \tag{4.18}$$

Here s_j and $\bar{s}_j$ are the numbers of vibrational degrees of freedom for the ion and the neutral, respectively; r_j and $\bar{r}_j$ are the corresponding numbers for the rotational degrees of freedom; and g_j and $\bar{g}_j$ are the electronic degeneracies. The different powers (4.17) and (4.18) result from the inclusion of the translational degrees of freedom in calculating $\bar{\rho}_{ij}$. Further, the factors a_j appearing in front of the zero-point energy $E_{0j} = \frac{1}{2}\sum_{\alpha=1}^{s_j} h\nu_{\alpha j}$ depend on the approximation used[28]: for the classical model $a_j = 0$; for the semiclassical Rice–Markus model $a_j = 1$; and in the Whitten–Rabinovitch formula a_j depends on E_j and the molecular frequencies $\nu_{\alpha j}$. The rotational factors Q_j and $\bar{Q}_j$ are given by[28]

$$Q_j = \frac{1}{\sigma_j}\left(\frac{8\pi^2}{h^2}\right)^{r_j/2} \pi^{d_1/2} \prod_{\alpha=1}^{r_j} I_{\alpha j}^{1/2} \tag{4.19}$$

and involve the inertial moments $I_{\alpha j}$ and the symmetry numbers σ_j. In dealing with the rotations we treat any three-dimensional rotation as two independent one- and two-dimensional rotations. For a nonlinear ion with $r_j = 3$ we therefore included in Eq. (4.19) an additional factor $\pi^{d_1/2} = \pi^{1/2}$. Similar relations apply to the neutral. For atomic species, Eqs. (4.17) and (4.18) reduce to

$$\rho_j(E) = g_j, \quad \bar{\rho}_{ij}(E) = \bar{g}_j E^{1/2}. \tag{4.20}$$

V. STATISTICAL MODEL CALCULATIONS

In this section we report phase space model calculations for the MPI fragmentation of benzene. The numerical results refer to the AMF model, i.e., we assume that all the energy available for fragmentation was already present in the parent ion $C_6H_6^+$. Actually, our discussion of the primary fragmentation rates under typical conditions realized in MPI experiments and of the spectra of some intermediates lead us to conclude that a more realistic model would involve multiple absorption and fragmentation steps. On the other hand, we do not have sufficient spectroscopic information to put such a MAF model on a quantitative basis. The strategy followed here will therefore be to show that a statistical description of the fragmentation is in close agreement with experiment. An essential test will be to predict the observed fragments and their probabilities as a function of laser intensity. With the picture of the MPI fragmentation following from the AMF phase space model, it is also possible to draw qualitative conclusions with respect to the somewhat more general MAF phase space model.

Before proceeding we make a few remarks on the calculations. We do not expect that phase space or any loose transition state theory predicts very reliable probabilities for H_2 eliminations, since the transition complex should on the contrary be rather of the tight type. In some cases the products phase space model incorrectly predicts a predominance of H_2 elimination over H abstraction. Most likely, an improvement should be obtained for any statistical approach applied to a more realistic transition state (e.g., by an RRKM model). In particular, this applies for H_2 eliminations of $C_4H_4^+$ and $C_3H_3^+$, which were assumed to have three-membered ring structures while the products $C_4H_2^+$ and C_3H^+ are linear. In view of the rather low probabilities for H_2 eliminations, as judged by Fig. 1, we deliberately decided not to include such processes in our calculation. Also, paths involving C_5 species were not included since their importance in MPI fragmentation of benzene is rather minor. Another point are fragmentations related by a charge transfer, e.g., $A^+ \rightarrow B^+ + C$ and $A^+ \rightarrow C^+ + B$. Using the rather analogous situation with a $(BC)^+$ collision complex in CA experiments, we chose only to retain the channel with the lower threshold, i.e., the outcome is $B^+ + C$ when B^+ has a smaller recombination energy than C^+. Finally, in calculating the densities of states by Eq. (4.17), the required molecular frequencies were available only in a few cases from spectroscopy.[27] For the majority of the ions and some of the neutrals, estimates were obtained by making some reasonable assumption on the molecular structure and using the average group frequencies of the bonds involved.[27,36] The geometric means of the frequencies needed in Eq. (4.17) are listed in Table III. Further, we have set the threshold energies equal to the enthalpies of reactions.

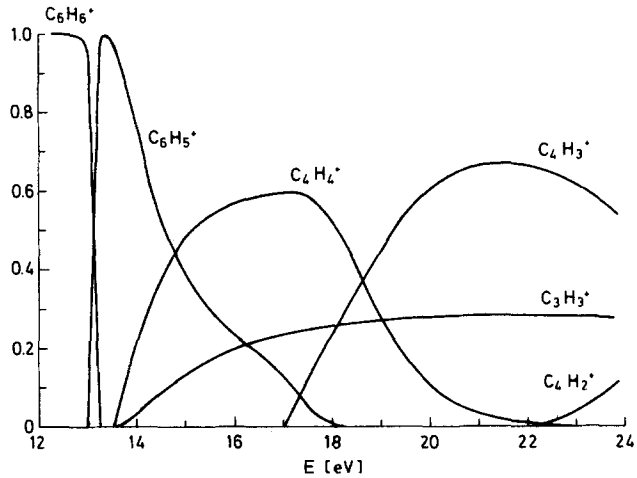

FIG. 3. Breakdown diagram of $C_6H_6^+$ obtained from the phase space model. The energy scale is as in Fig. 1.

Two findings support our view that MPI fragmentation may in fact proceed by multiple fragmentation steps with branchings competing according to our statistical model:

First, the breakdown graph of benzene up to energies of about 10 eV above the ionization limit (Fig. 1) can serve as a check of the phase space model. By the experimental situation in CA and PI studies, any secondary excitation of the fragments by photons or collisions is ruled out. Our result (Fig. 3) is in good agreement and shows for instance that formation of $C_6H_5^+$ is important only at rather low energies. Above its slightly higher threshold $C_4H_4^+$ becomes predominant. Also, the ratio $C_4H_4^+/C_3H_3^+ \sim 3$ agrees with the experimental observation. Remaining discrepancies between Figs. 1 and 3 are due to the neglect of H_2 eliminations by which we underestimate $C_6H_4^+$ and $C_4H_2^+$ and the "infinite-detection-time"

TABLE III. Ions and major fragmentations predicted by the phase space model used in this work.

Ion	ν (cm^{-1})[a]	Fragments $C_mH_n^+$;[b] thresholds in eV	A. P. (eV)[c]
$C_6H_6^+$		65(3.8); 44(4.3); 33(4.5)	9.25
$C_6H_5^+$	1179	43(4.1); 23(5.0); 44(5.4); 41(5.7); 64(5.9); 42(6.3); 31(6.8)	13.0
$C_6H_4^+$	1142	42(2.2); 43(3.0); 22(3.4); 41(4.3); 31(4.7)	18.9
$C_4H_4^+$	1143	43(3.5); 22(4.1); 23(4.6); 33(5.2); 31(5.9)	13.6
$C_4H_3^+$	1078	42(4.0)	17.1
$C_4H_2^+$	812	41(3.9); 31(7.6)	19.3
C_4H^+	743	31(7.2); 40(8.4); 20(8.9); 30(10.3)	18.7
C_4^+	629	10(4.3); 20(6.4)	27.0
$C_3H_3^+$	1252	32(6.6); 23(8.0); 22(8.8)	13.7
$C_3H_2^+$	956	31(3.3); 21(8.0); 20(9.2)	20.4
C_3H^+	812	30(6.6); 21(8.2); 20(10.3)	19.5
C_3^+	760	10(6.5)	26.0
$C_2H_3^+$	1586	22(4.3)	18.0
$C_2H_2^+$	1225	21(5.8)	17.6
C_2H^+	1300	20(5.6)	23.4
C_2^+	1350	10(5.4)	27.5
C^+			31.3

[a]Gecmetric mean frequencies $\nu_j = (\Pi^{s_j} \nu_{\alpha_j})^{1/s_j}$ for complementary neutrals: C_4H_2 (819.); C_3H_4 (1238.); C_3H_2 (1211.); C_3 (760.); C_2H_4 (1586.); C_2H_3 (1586.); C_2H_2 (1235.); C_2H (1349.); C_2 (1855.); CH_3 (2072.); CH_2 (2049.); CH(2858.).

[b]The notation used is for example, 65 for $C_6H_5^+$.

[c]Minimal appearance potentials for the fragmentation tree which includes only the branchings according to this Table.

limit inherent in our model. When compared with the experimental situation, this shifts the onset of the fragmentations to lower energies by about 1 eV. With respect to the RRKM model used to interpret the primary fragmentation steps of benzene ions,[11] one therefore concludes that the phase space approach followed here is equally valid.

Second, one can apply the phase space model to the very general fragmentation tree discussed in Sec. III and assign relative probabilities to the rather huge number of conceivable sequences. Table III lists only those fragments with overall probabilities above 1% when we studied separately the fragmentations of all molecular ions of Table II. By this the number of sequences is considerably reduced. However, even more important is that the surviving fragments are exactly those which are observed in MPI experiments. Thus, despite of the rather similar appearance potentials (Table II), the statistical theory very strongly discriminates against ions like CH^+ and CH_2^+ by giving a small statistical weight to all paths by which they could be formed.

In the calculations we scanned a range of $C_6H_6^+$ energies E up to around 100 eV. An example of a series of energy distributions $P_j(E_j)$ in Eq. (4.11) for the molecular fragments prior to fragmentation is shown in Fig. 4 for $E = 60$ eV. Thereby one is able to easily follow the major routes of fragmentation and further one obtains a quantitative picture of the energy content in the ions.

In Fig. 5 we show the mass distributions P_j in Eq. (4.12) calculated by the AMF phase space model for three energies. One sees that the formation of smaller ions becomes efficient only at energies much above the minimal energies calculated from the threshold energies. The C^+ peak becomes notable for parent ion energies

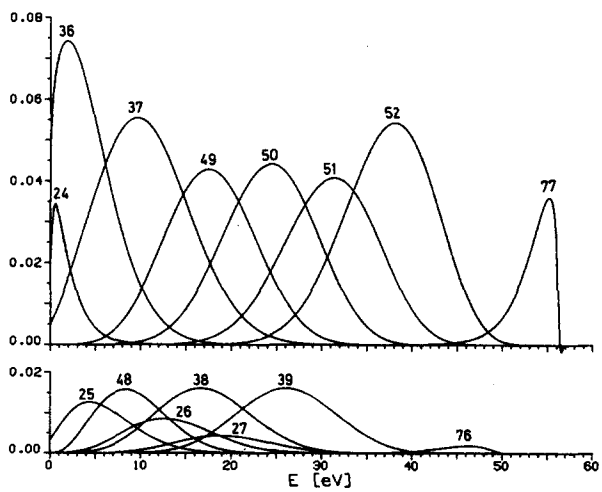

FIG. 4. Energy distributions $P_j(E)$ prior to fragmentation for masses 77 ($C_6H_5^+$), 76 ($C_6H_4^+$), 52 ($C_4H_4^+$), 51 ($C_4H_3^+$), 50 ($C_4H_2^+$), 49(C_4H^+), 48 (C_4^+), 39 ($C_3H_3^+$), 38 ($C_3H_2^+$), 37 (C_3H^+), 36 (C_3^+), 27($C_2H_3^+$), 26 ($C_2H_2^+$), 25 (C_2H^+), and 24 (C_2^+). The initial excess energy of $C_6H_6^+$ is 60 eV.

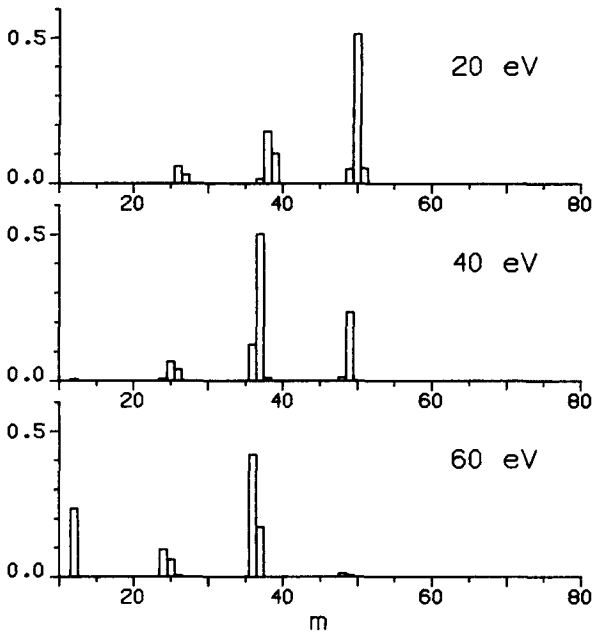

FIG. 5. Mass distributions for energy-selected benzene ions predicted by the AMF phase space model for various excess energies of $C_6H_6^+$.

around 40 eV, whereafter it increases rapidly in intensity. For energies above 60 eV, C^+ becomes the most abundant ion. The major path leading to it is the sequence $C_6H_6^+ \rightarrow C_4H_4^+ \rightarrow C_4H_3^+ \rightarrow C_4H_2^+ \rightarrow C_4H^+ \rightarrow C_3H^+ \rightarrow C_3^+ \rightarrow C^+$ and requires a minimum energy content in the parent ion of 36 eV. Other C_1 fragment ions such as CH^+ and CH_2^+ have very small probabilities < 0.003.

To make a closer connection of the calculated mass patterns vs energy with the experimental MPI fragmentation spectra, we need the distribution $P(E)$ of the energy in the parent ion as a function of the laser output. We refer to a model by Reilly and Kompa[2] used to reproduce the total ion yield for benzene in MPI by ArF and KrF lasers by the following rate equations:

$$\frac{d[C_6H_6(^1B_{1u,2u})]}{dt} = \sigma_1 I[C_6H_6] - [(\sigma_2+\sigma_3)I + 1/\tau][C_6H_6(^1B_{1u,2u})], \qquad (5.1)$$

$$\frac{d[C_6H_6^+]}{dt} = \sigma_2 I[C_6H_6(^1B_{1u,2u})] ,$$

where $I = I(t)$ is the photon flux density and the other parameters were $\sigma_1 = \sigma_3 = 0.0033$ Å^2, $\sigma_2 = 0.34$ Å^2, and $\tau = 50$ nsec at 248 nm, i.e., for the KrF laser. Benzene ions formed from benzene after the absorption of two KrF photons via the intermediate $^1B_{2u}$ state would arise with a slight excess energy ΔE of less than 1 eV. According to our AMF model and the assumption of fast radiationless transitions by which excited $C_6H_6^+$ states pump vibrational energy into the $C_6H_6^+$ ground state, we obtain a crude estimate for the relative probabilities for benzene ions that have absorbed n photons during the pulse by adding a set of equations

$$\frac{d[C_6H_6^+(n)]}{dt} = \sigma_4 I\{[C_6H_6^+(n-1)] - [C_6H_6^+(n)]\} , \quad n \geq 1 . \qquad (5.2)$$

Here σ_4 was guessed to be 0.02 Å^2 independent of n and further a Gaussian time profile of the laser pulse was taken. For the initial benzene pressure we set 5×10^{-6} Torr. The energy distribution of the benzene ions is then

$$P(E) = \sum P_n \delta(nh\nu + \Delta E) , \qquad (5.3)$$

where

$$P_n = \frac{[C_6H_6^+(n)]}{\sum[C_6H_6^+(n)]} \qquad (5.4)$$

is given by the ion densities at the end of the pulse. In Fig. 6 we show a set of mass spectra obtained from the single-energy phase space results after averaging with $P(E)$ given by Eq. (5.3).

Clearly, there is evidence enough that major features of the experimental mass spectra are correctly reproduced by our calculation. First, the fragmentation occurs in the range of laser intensities or fluences where it is also experimentally observed. Other points are of course the dominance of smaller fragments with increasing laser intensity that could have already been anticipated from the single energy results. The only C_1 fragment ion is C^+, which increases rapidly above some threshold to become the most important species at fluences above 5 J/cm^2. For comparison, Fig. 7 shows experimental MPI fragmentation patterns. When looking at the relative probabilities within a group of C_n fragments ($n = 2, 3, 4$), we again note the general tendency of consecutive loss of H atoms with increasing laser intensity. One might further mention the low abundance of C_4^+ at all intensities, which is related to the high threshold for $C_4H^+ \rightarrow C_4^+$. Eventually, it can be argued that our calculation underestimates the C_2 fragments and in particular $C_2H_3^+$. However, we feel that more accurate data on the thermochemical and spectroscopic input used in the model are required before such details can be discussed.

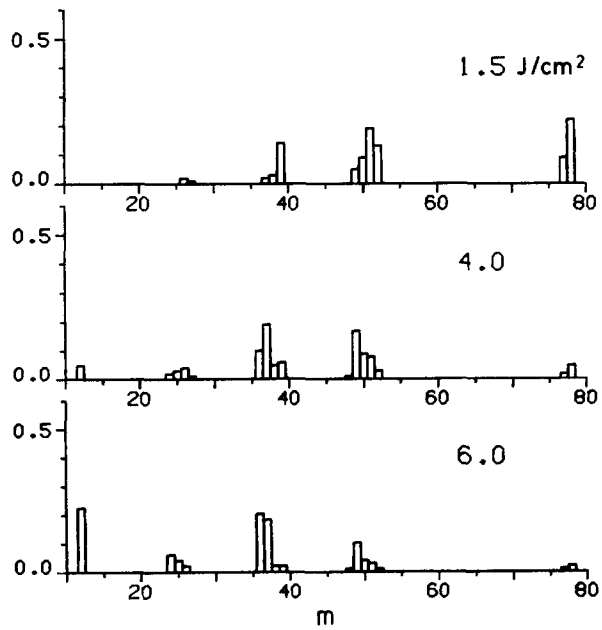

FIG. 6. Mass distributions for MPI fragmentation of benzene vs laser fluence obtained by the AMF phase space model.

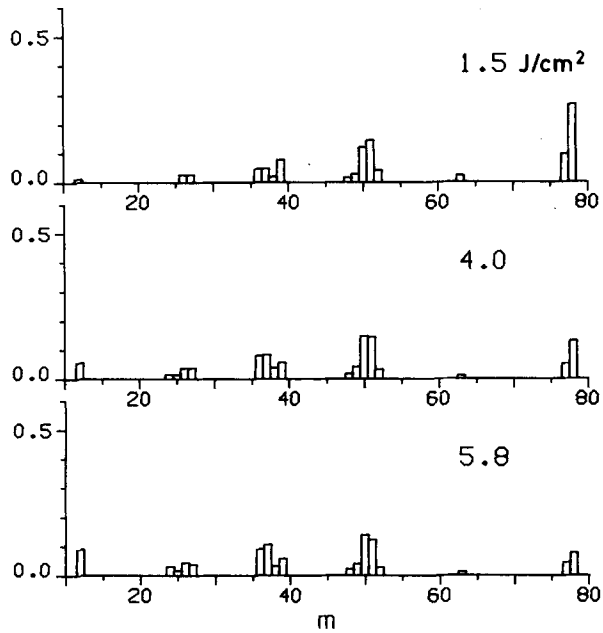

FIG. 7. Mass distributions for MPI fragmentation of benzene vs laser fluence observed in KrF laser experiments by Reilly and Kompa.[2]

As a final point, we would like to come back to the question of secondary absorption by some of the fragments. Necessarily, the AMF phase space model must overestimate the energy content of the parent ions. Energy distributions prior to fragmentation (Fig. 4) show quite clearly that much of the excess energy is already lost in the early fragmentation steps. For instance, in the case of the $C_6H_6^+ - C_4H_4^+$ channel the energy content of the $C_4H_4^+$ is roughly $\frac{2}{3}$ of the excess energy in the parent ion, in agreement with equipartition among all degrees of freedom. The smaller the neutral fragment, the more energy can be routed to the ionic fragment, extreme cases being H abstractions where only the bond energy and the relative translational energy determine the loss. In general, the effect of absorption of photons in driving the fragmentation increases the later it occurs in a particular sequence. Natural limits are set by the duration of the pulse and spectroscopic properties. To the extent that effective branching ratios of all species already present during the pulse are not too strongly affected by their energy content, the MAF model would predict the onsets of smaller fragments to occur at somewhat lower laser intensities. One also imagines compensating effects, e.g., due to lower absorption rates in the smaller ions. Apart from the different mode of energy aquisition, qualitative and quantitative predictions by the AMF or MAF models may therefore in fact be rather similar.

VI. CONCLUDING REMARKS

Very recently, Silberstein and Levine[37] analyzed MPI fragmentation patterns of benzene by a different, but also statistical, approach. Mass and energy distributions of all fragments were calculated by maximizing the entropy of a $(6C + 6H)^+$ system subject to the constraints of mass and charge conservation and given average energy. The energy of all molecular fragments is Boltzmann distributed with a temperature determined from the average laser energy absorbed by the system. The higher this temperature, the more extensive is the fragmentation to smaller species, in good agreement with the available experimental data.

Our approach (Secs. IV and V) emphasizes the mechanistic aspects of MPI fragmentation. In particular, we attempt to identify the important fragmentation paths and the mode of energy acquisition. Statistics comes in by assigning weights to the various sequences of a rather general fragmentation tree by the phase space volume of the products. Comparing experimental and calculated results, it was concluded that such a statistical approach to MPI fragmentation provides a reasonable model even on a quantitative level. Because of its mechanistic content, our model can be made subject to further experimental tests, e.g., on the direct (independent of the ionization step) laser fragmentation of $C_6H_6^+$ or any of the intermediates. Of interest also will be to check similar models for other polyatomics. For the MPI fragmentation of acetaldehyde, Fisanick *et al.*[38] investigated a kinetic scheme based on direct photoionizations from a resonant neutral state to various product ions and consecutive photodissociations of the ions formed. In contrast, our model claims that for C_6H_6 photoionization leads to energy-rich parent ions which fragment from the ground state, according to statistical theory. Similarly, we view the photodissociation processes discussed for the MAF model.

The phase space model used in this work intends to be valid when absorption and fragmentation are rate limiting factors of the overall MPI fragmentation process, while others like radiationless transitions or energy randomization proceed rapidly enough to ascertain the applicability of statistical theories. With the present standard in laser technique, it seems possible to realize experimental situations with different orderings of the relevant time scales, e.g., by employing picosecond laser pulses of high power.[39]

ACKNOWLEDGMENTS

The authors acknowledge gratefully discussions with Ch. Lifshitz, K. L. Kompa, K. Hohla, and R. D. Levine during the course of this work.

[1] S. Rockwood, J. P. Reilly, K. Hohla, and K. L. Kompa, Opt. Commun. **28**, 175 (1979).
[2] J. P. Reilly and K. L. Kompa, J. Chem. Phys. **73**, 5468 (1980).
[3] L. Zandee and R. B. Bernstein, J. Chem. Phys. **70**, 2574 (1979).
[4] L. Zandee and R. B. Bernstein, J. Chem. Phys. **71**, 1359 (1979).
[5] U. Boesl, H. J. Neusser, and E. W. Schlag, Z. Naturforsch. Teil A **33**, 1546 (1978).
[6] U. Boesl, H. J. Neusser, and E. W. Schlag, J. Chem. Phys. **72**, 4327 (1980).
[7] D. M. Lubman, R. Naaman, and R. N. Zare, J. Chem. Phys. **72**, 3034 (1980).
[8] V. S. Antonov, V. S. Letokhov, and A. N. Shibanov, Appl. Phys. **22**, 293 (1980).
[9] B. Andlauer and Ch. Ottinger, J. Chem. Phys. **55**, 1471 (1971); Z. Naturforsch. Teil A **27**, 293 (1972).

[10]J. H. D. Eland and H. Schulte, J. Chem. Phys. **62**, 3835 (1975); J. H. D. Eland, R. Frey, and B. Brehm, Int. J. Mass. Spectrom. Ion Phys. **21**, 209 (1976).
[11]T. Baer, G. D. Willett, D. Smith, and J. S. Philips, J. Chem. Phys. **70**, 4076 (1979).
[12]B. S. Freiser and J. L. Beauchamp, Chem. Phys. Lett. **35**, 35 (1975); T. E. Orlowski, B. S. Kreiser, and J. L. Beauchamp, Chem. Phys. **16**, 439 (1976).
[13]B. O. Jonsson and E. Lindholm, Ark. Fys. **39**, 65 (1967).
[14]A. C. Parr, A. J. Jason, and B. Stockbauer, Int. J. Mass. Spectrom. Ion Phys. **33**, 243 (1980).
[15]A. C. Parr, A. J. Jason, and R. Stockbauer, Int. J. Mass. Spectrom. Ion Phys. **26**, 23 (1978).
[16]A. C. Parr, A. J. Jason, R. Stockbauer, and K. E. McCulloh, Int. J. Mass. Spectrom. Ion Phys. **30**, 319 (1979).
[17]M. Gerard, T. R. Govers, and R. Marx, Chem. Phys. **30**, 75 (1978).
[18]J. H. D. Eland, Int. J. Mass. Spectrom. Ion Phys. **31**, 161 (1979).
[19]I. Szabo and P. J. Detrick, Int. J. Mass Spectrom. Ion Phys. **7**, 55 (1971).
[20]W. Wagner, K. Levson, and Ch. Lifshitz, Org. Mass Spectrom. **15**, 271 (1980).
[21]A. Hustrulid, P. Kush, and J. T. Tate, Phys. Rev. **54**, 1037 (1938).
[22]A. Cornu and B. Massot, *Compilation of Mass Spectral Data* (Heyden, London, 1979).
[23]K. R. Jennings, Z. Naturforsch. Teil A **22**, 454 (1967).
[24]H. M. Rosenstock, K. Draxl, B. W. Steiner, and J. T. Herron, J. Phys. Chem. Ref. Data **6**, Suppl. 1 (1977).
[25]J. L. Franklin, J. G. Dillard, H. M. Rosenstock, J. T. Herron, and K. Draxl, Natl. Stand. Ref. Data Ser. Natl. Bur. Stand. **26** (1969).
[26]See, for example, R. C. Dunbar, in *Gas Phase Ion Chemistry*, edited by M. T. Powers (Academic, New York, 1979).
[27]G. Herzberg, *Molecular Spectra and Molecular Structure* (Van Nostrand, New York, 1958), Vol. I–III.
[28]G. Forst, *Theory of Unimolecular Reactions* (Academic, New York, 1973).
[29]W. J. Chesnavich and M. T. Bowers, in Ref. 26.
[30]Ch. Lifshitz, Adv. Mass Spectrom. A **7**, 3 (1978).
[31]See, for example, R. D. Levine and A. Ben-Shaul, *Chemical and Biochemical Applications of Lasers*, edited by C. B. Moore (Academic, New York, 1977), Vol. II, Chap. 4; A. Ben-Shaul, R. D. Levine, and R. Bernstein, J. Chem. Phys. **61**, 4537 (1975); A. Ben-Shaul, Chem. Phys. **22**, 341 (1977).
[32]C. E. Klots, J. Phys. Chem. **75**, 1526 (1971).
[33]P. Pechukas and J. C. Light, J. Chem. Phys. **42**, 3281 (1965).
[34]E. E. Nikitin, Theor. Exp. Chem. (USSR) **1**, 83 (1965).
[35]R. A. Marcus, J. Chem. Phys. **45**, 2138, 2630 (1966).
[36]T. Shimanouchi, Tables of Molecular Vibrational Frequencies, Natl. Stand. Ref. Data Ser. Natl. Bur. Stand. **39**, (1972).
[37]J. Silberstein and R. D. Levine, Chem. Phys. Lett. **74**, 6 (1980).
[38]G. J. Fisanick, T. S. Eichelberger, B. A. Heath, and M. B. Robin, J. Chem. Phys. **72**, 5571 (1980).
[39]P. Hering, A. G. M. Maaswinkel, and K. L. Kompa, Chem. Phys. Lett. (to be published).